Proceedings of the ASME 2010 3rd Joint US-European Fluids Engineering Summer Meeting and 8th International Conference on Nanochannels, Microchannels, and Minichannels
FEDSM-ICNMM2010
August 1-5, 2010, Montreal, Canada

FEDSM-ICNMM2010-30498

EXPERIMENTAL INVESTIGATION OF THE WAKE OF A DISCONTINUOUS CYLINDER

V. S. R. Mandava
Universitat Rovira i virgili
Department d'Enginyeria quimica
Tarragona, Cataluña, Spain

Gregory A. Kopp
University of Western Ontario
Faculty of Engineering
London, Ontario, Canada
e-mail: gakopp@uwo.ca

Joan Herrero
Universitat Rovira i Virgili
Department d'Enginyeria quimica
Tarragona, Cataluña, Spain

Francesc Giralt
Universitat Rovira i Virgili
Department d'Enginyeria quimica
Tarragona, Cataluña, Spain
e-mail: fgiralt@urv.cat

ABSTRACT

The effects of a discontinuous cylinder geometry on the near wake structures was investigated experimentally. This 'discontinuous' circular cylinder has gaps so that solid segments 5D long are followed by gaps 2.5D long, in a repeating pattern, where D is the diameter of the cylinder. A thin steel plate was used to hold all of the cylinder pieces together. Thus, a three-dimensional (3D) wake was created at the origin with the intent to force the near wake flow to have similar structural characteristics as the far wake behind an 'infinite/continuous' cylinder, i.e., a near wake flow with horseshoes or double rollers formed by rapid kinking of Kármán-like vortices. Since the kinetic energy associated with the fluctuations of these near-wake 3D vortical structures is high, the flow system is considered suitable to clarify the role of these velocity patterns in the entrainment process of wake flows, which is still the subject of controversy. Particle Image Velocimetry (PIV) and Hot-Wire Anemometry (HWA) techniques were used to analyze the flow at two Reynolds numbers, Re=10000 and 4000, in the wake of the discontinuous cylinder up to x/D=190 downstream. The development of double rollers resulting from the interaction between the high momentum flow through the gaps and the Kármán-like vortices formed behind the solid cylindrical segments was confirmed. The Strouhal number of the double rollers in the wake is 0.14. These vortices have a dominant role in the initial wake growth. Thus, the overall flow dynamics are similar to the momentum transfer that takes place at the scale of the intermittent turbulent bulges that protrude from the wake in the far region and that were reported to be associated with double rollers.

INTRODUCTION

Understanding the kinematics and dynamics of entrainment and mixing is important in many practical engineering situations. Entrainment has been considered by many researchers as a large-scale process, e.g., [1,2] and several phenomenological descriptions have been proposed in the past. Examples are the vortex sheet roll-up due to a Kelvin-Helmholtz instability and entrapment of external fluid into the core of the vortex [3-5]; Townsend´s growth-decay model [1,6]; 'sweeping' non-turbulent fluid into the turbulent region by rotational motions [2]. These theories or phenomenological models do not explain the role of large scale vortical structures in relation to the initial conditions that generate them. In contrast to the large-scale approaches to entrainment just mentioned, Mathew and Basu [7] and Westerweel et al. [8] concluded that the mechanism of entrainment process is dominated by small scales (nibbling). Thus, it is still not clear whether the entrainment process occurs as a result of outward spreading of small-scale vortices by "nibbling" or by the action of large-scale eddies in the region of the turbulent-nonturbulent interface.

Wakes are an ideal flow system to study the genesis of large scale vortices and their dynamical evolution with respect to initial flow conditions. The instability and transition in the near wake has been studied by many researchers [9-15]. Several numerical and experimental studies have also been carried out in the past to characterize the three-dimensional (3D) nature of wake flows and vortex shedding by exciting 3D modes at the originating body, e.g., [16-22]. A more radical initial perturbation in a 2D wake flow behind a continuous/infinite body in the spanwise direction could be attained by alternating solid with discontinuous segments of the same body in a repeating pattern. This would have the benefit of not changing the basic body geometry that generates the wake flow.

In the current study, we have considered a 3D cylinder configuration with gaps, i.e., segments of equidistant cylinders along the cylinder center axis. With this arrangement, part of the free stream flow passes through the gaps while the rest passes over the 3D cylinder segments, forming a 3D wake. The free stream flow through the gaps would move inwards towards each wake behind the cylindrical segments due to the pressure gradients. Simultaneously, Kármán-like vortices would be formed behind the solid segments together with other vortical structures at both ends. This new configuration of the initial flow conditions should cause kinking of the segmented, 3D Kármán-like vortices with horseshoe/double-rollers vortices generated in the near wake. These are the vortices that usually occur in the far wake region behind a continuous/infinite cylinder, e.g., [23-26]. As a consequence, the current flow configuration may induce the generation of double rollers early in the wake and show how they evolve with respect to initial flow conditions.

NOMENCLATURE

All lowercase letters represents the mean flow variables and they are also normalized with free-stream velocity (U) and cylinder diameter (D)

D	Diameter of a cylinder piece (m)
U	Free stream velocity (m/sec)
u	Stream-wise velocity
v	Transverse velocity
w	Span-wise velocity
u′	Stream-wise root mean square velocity
u′u′	Stream-wise normal stress
u′v′	Shear stress on x-y plane
u′w′	Shear stress on x-z plane
v′	Transverse root mean square velocity
v′v′	Transverse normal stress
ω_y	Transverse vorticity
ω_z	Span-wise vorticity
$y^{1/2}$	wake half-width

EXPERIMENTAL DETAILS

Preliminary experiments were carried out in a small open-return wind tunnel at the Boundary Layer Wind Tunnel Laboratory (BLWTL), University of Western Ontario, Canada, while the majority of the experiments were conducted in the open return wind tunnel of the Chemical Engineering Department at the Universitat Rovira i Virgili in Tarragona. In both wind tunnels, measurements were conducted with the same discontinuous cylinder model and at the same free-stream velocity, U = 9.2m/s, thus, at the same Reynolds number Re = 10^4. The diameter (D) of the cylinder pieces was 0.0163m, the length of each segment was 5D, and the gap between the cylinder pieces was 2.5D. A thin steel plate, whose thickness was 0.81mm and width equal to the cylinder diameter, held the cylindrical pieces together without interfering significantly with the flow between the gaps. The dimensions of the model and co-ordinate system used are shown in Fig. 1. At Re = 10^4, the boundary layer on the cylinder surfaces is laminar, while the wake is fully turbulent [27]. Particle image velocimetry (PIV) was used to measure the instantaneous velocity field in the wake region.

First, several measurements were conducted in Canada, in the near wake region up to 8.5 diameters downstream on transverse (x-y) planes, along the cylinder axis. Planes at every half a diameter width, from center of the middle cylinder piece (z/D=0) to the end of the middle cylindrical section (z/D=2.5), were examined. Two measurements were carried out within the gap region between cylindrical section, one at 0.5D away from the edge of the cylinder piece (i.e., at z/D=3.0) and the other at the center of the gap region (z/D=3.75). Several experiments were carried out on transverse(x-y) planes to check flow symmetry.

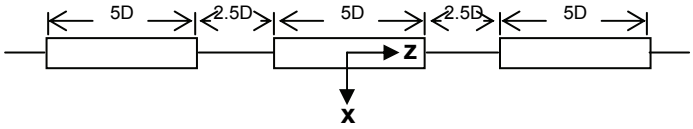

Figure 1. Cylinder model and co-ordinate system; y is vertical upwards for a normal right-handed Cartesian coordinate system

The experiments were repeated with stereo particle image velocimetry in Tarragona, Spain, with the same discontinuous cylinder configuration (Fig. 1) but with five cylinder segments, instead of the three in the earlier setup. The data obtained were in agreement, within the measurement uncertainty, with the earlier experimental data obtained in Canada.

Measurements in Tarragona extended further downstream in the wake at several vertical (x-y) planes, x/D=9 to 16, 26 to 36, 43 to 56, 70 to 90, 110 to 130, and 170 to 190, in the central plane of the discontinuous cylinder (z/D=0). Experiments were also conducted in the horizontal (x-z) planes in the wake, from x/D=10 to 20 at y/D=2, and 27 to 36 at y/D=3. All PIV experiments up to x/D=56 downstream wake were conducted at flow Reynolds

number Re=10000 and the experiments in the wake further downstream were carried out at the Reynolds number Re=4000. Data for the corresponding wake of an infinite cylinder were also collected in the same vertical and horizontal planes. The aspect ratio of the infinite cylinder was 37 and the blockage in the tunnel was 2.7%. TSI Insight 3G software was used, in all cases, for frame to frame correlation to generate instantaneous velocity fields, with an interrogation window of size 32 x 32 pixels with 50% overlap. These instantaneous velocity fields were then ensemble averaged to determine the mean streamwise and transverse velocities, root mean square (r. m. s) velocity fluctuations, mean Reynolds shear stresses and mean z-vorticity patterns on all the transverse (x-y) and horizontal (x-z) planes. The instantaneous data on horizontal planes were used to identify the footprints of double rollers in the near wake.

Hot-wire anemometry (HWA) experiments were also carried out at several downstream stations (x/D=12, 16, 26, 52, 76, 120, 170 and 190), in the near and far wake regions of the wake at Reynolds number Re=4000. A horizontal rake, which is movable on transverse axis, was placed parallel to spanwise axis in the wake. The rake consists of three normal wire probes, positioned at the center of the middle cylinder piece (z/D=0), at the end of the middle cylinder piece (z/D=2.5) and at the center of the gap region (z/D=3.75), respectively, and was used to collect the streamwise velocity (u) data at three spanwise locations simultaneously. At every downstream station, the rake was moved on transverse axis and collected data from middle of the wake (y/D=0) to the outer edge of the wake. The used spatial resolutions on transverse axis were different from near wake to the far wake and are shown in table 1. At all points, the data were acquired for 120sec at a sampling rate of 5 kHz and low pass filtered at 2 kHz and stored on a computer for subsequent processing. These data are used to show the spectra and the evolution of mean and rms (root-mean–square) values of the fluctuations of the stream-wise velocity. The data were also used to verify the consistency of the PIV data.

Down stream station (x/D)	Spatial resolution (Spacing/D)
12	0.11
16	0.11
26	0.15
52	0.23
76	0.31
120	0.38
170	0.46
190	0.46

Table 1. Spatial resolution on transverse axis at different downstream stations.

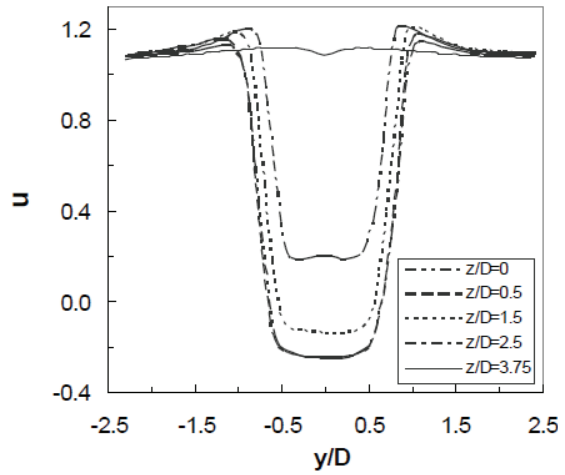

(a)

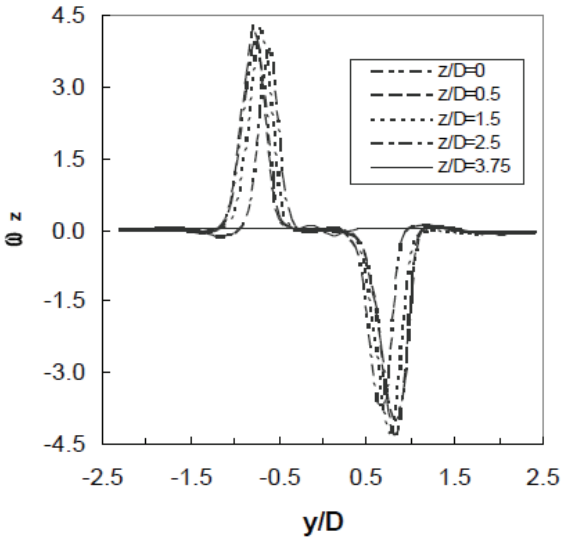

(b)

Figure 2. (a) Profiles of mean streamwise velocity (u) at x/D=1; (b) profiles of mean z-vorticity (ω_z) at x/D=1

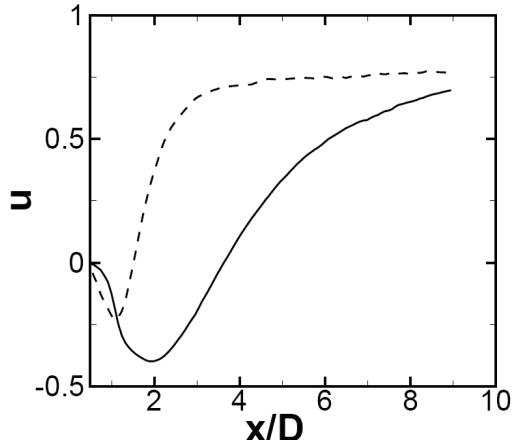

Figure 3. Mean streamwise velocity (u) on wake centerline (y/D=0) of discontinuous (—) and continuous (----) cylinders

WAKE CHARACTERISTICS

Current data for the continuous/infinite cylinder were compared and found in reasonable agreement with measurements reported in the literature [15,28]. In the following sections, discontinuous and infinite cylinder data are compared. The plots presented in the paper are, unless specified, on transverse planes at z/D=0. In all contour plots flow direction is from left to right and, positive and negative magnitude of contours are indicated by solid and dashed lines, respectively.

For the discontinuous cylinder case, note that the velocity defect and vorticity levels in the wake downstream of the gaps are much smaller than those in the wake directly behind each cylindrical section (Fig. 2).

The vortex formation length is defined as the distance between the separation point and the location at which the vortex is fully formed [28-32]. The formation length for the wake for the discontinuous cylinder is 3.62D, and the corresponding value for the infinite cylinder is 1.5D in the present experiments, consistent with the result found by Norberg [28]. As used in Norberg [28], we have used time-averaged closure point (i.e., the saddle point on the wake centerline in Figure 3) to measure the formation length.

The mean streamwise velocities on the wake centerline (Fig. 3) show strong negative values (reversed flow) in the base region. The magnitude of the minimum velocity and the location where this occurs are different from the infinite cylinder case. The maximum magnitude of the negative velocity is 0.40 and the corresponding value for the infinite cylinder is 0.23 in the current experiments. The width of the wake at x/D=1.5 is much wider than the wake behind the infinite cylinder (Fig. 4a). The wake has a greater velocity deficit in the region close to the cylinder when compared to the infinite cylinder case, but as the wake grows downstream it recovers quickly (Fig. 4).

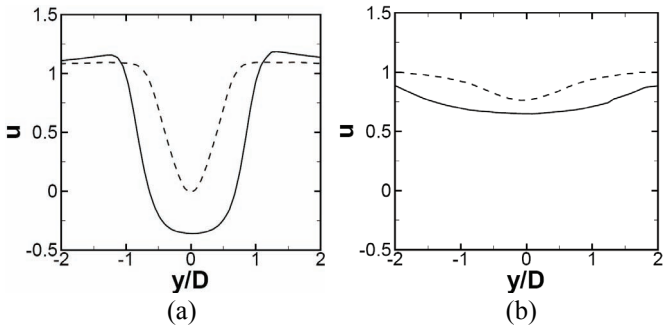

Figure 4. Comparison of mean streamwise velocity (u) in discontinuous (—) and continuous (----) cylinder wakes at (a) x/D=1.5; (b) x/D=8

The u′ and v′ are the streamwise and transverse rms velocities. The magnitude of the maximum fluctuations of the normalized rms streamwise velocity (u′) for the discontinuous cylinder is smaller. The corresponding location is displaced further downstream compared to the infinite cylinder case. The maximum value is 0.30 and occurs at x/D=2.5. The corresponding values for the infinite cylinder are 0.45 at x/D=1.4 from the current experiments.

ENTRAINMENT PROCESS

The horseshoe eddy is a structure with two legs which are shear aligned and connected at the top with spanwise vorticity. The cross-section of the two legs forms a double roller pattern on the horizontal plane [25,26]. These double roller structures, which are known to appear in the far wake region behind an infinite cylinder, are also observed in the near wake (x/D≈15) of the discontinuous cylinder, as shown in Fig. 5. The vectors of streamwise and spanwise velocity fluctuations on horizontal (x-z) plane clearly depict in this figure the footprints of double roller vortices early in the discontinuous wake development. Similar kind of double roller structures are found on the horizontal plane further downstream (x/D≈30) behind the discontinuous cylinder, as shown in Fig. 6.

The corresponding mean streamwise velocity (u) profiles at different downstream stations in the plane z/D=0 are shown below (Fig. 7). The profiles in the wake up to x/D=12 downstream are Gaussian (Fig. 4 & Fig. 7), while further downstream wake the profile has two minima, probably because of the rotation of the double rollers, which will input momentum close to the interface (lower defects with steeper u-velocity gradients) and a negative input closer to the center line (opposed rotation or the wake movement).

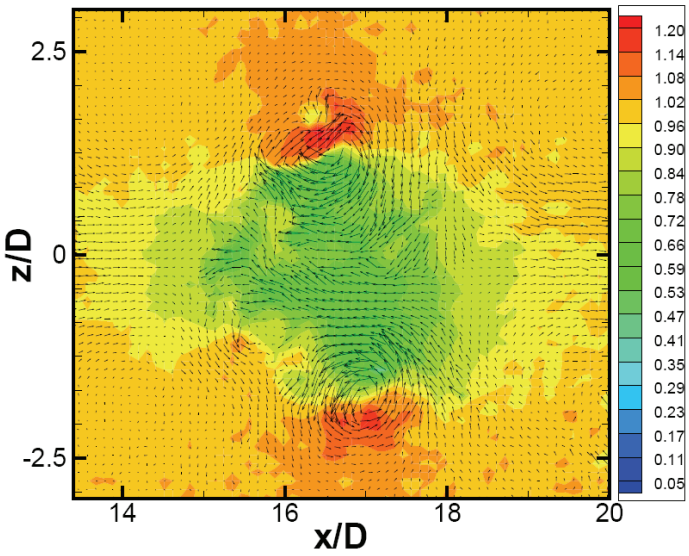

Figure 5. An example of normalized (u,w) velocity fluctuations and u velocity contours in the near wake behind the discontinuous cylinder, at y/D=2, showing double roller patterns.

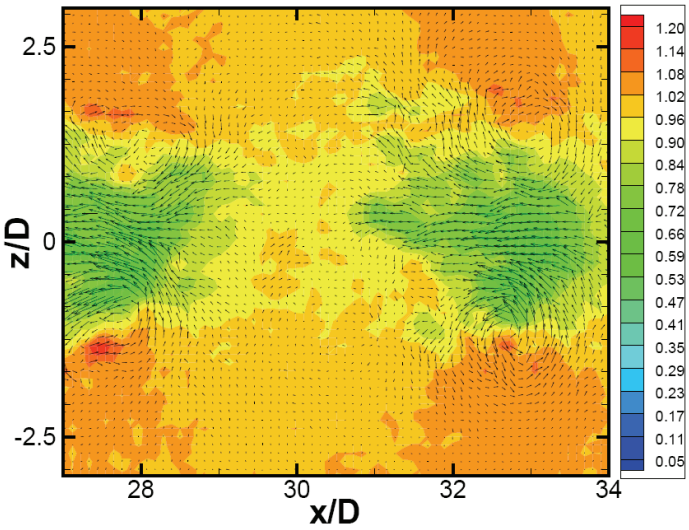

Figure 6. An example of normalized (u,w) velocity fluctuations and u velocity contours in the medium far wake behind the discontinuous cylinder, at y/D=3, showing double roller patterns.

The corresponding profiles of streamwise rms velocity fluctuations (u´) at several downstream stations are show in Fig. 8. At the downstream station, x/D=190, the peak in the profile almost disappears and the profile looks flat with very low fluctuation levels.

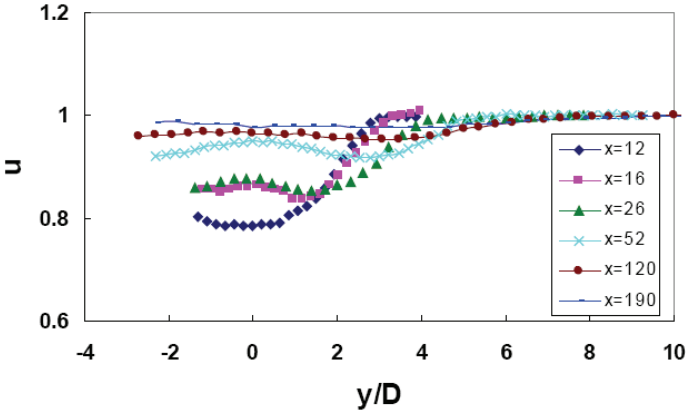

Figure 7. The profiles of mean streamwise velocity (u) at several downstream stations in the plane z/D=0

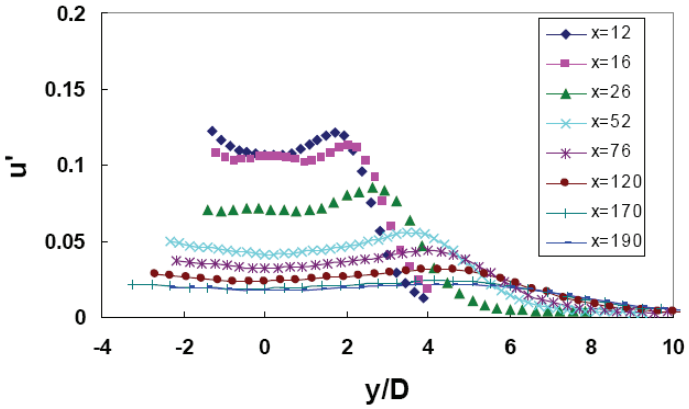

Figure 8. The profiles of rms streamwise velocity fluctuations in the plane z/D=0

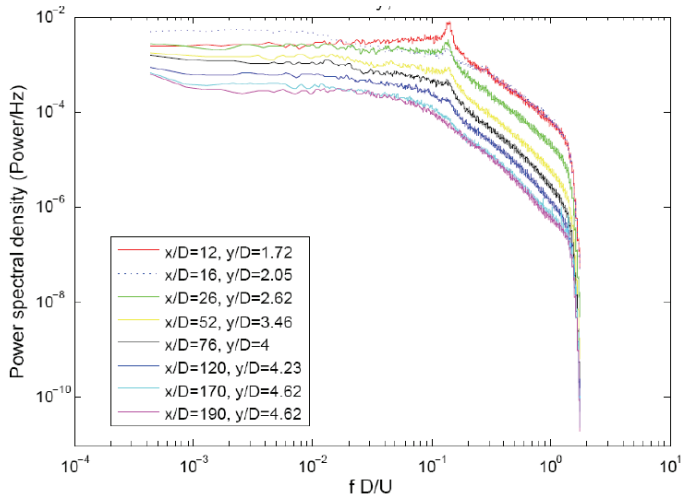

Figure 9. Spectra at different down stream stations in the plane z/D=0

The spectra at several down stream stations in the plane z/D=0 is shown in Fig. 9. It shows that the non dimensional shedding frequency (Strouhal number) of the dominant structures in the wake is 0.14. The corresponding value for the continuous cylinder wake is 0.2. The spectra also shows that the dominant structures in the wake have higher energy levels up to x/D=120, and further downstream in the wake they are comparable with the energy levels of the surrounding turbulent flow.

The corresponding spanwise profiles of mean y-vorticity and mean u'w' shear stresses are presented in Fig. 10. The Fig. 10a shows how the y-vorticity decreases with x/D as double rollers are advected downstream and diffused. The u'w' shear stress also diminishes with x/D (Fig. 10b), which is indicative of the wake evolution towards fully development (u´w´=0).

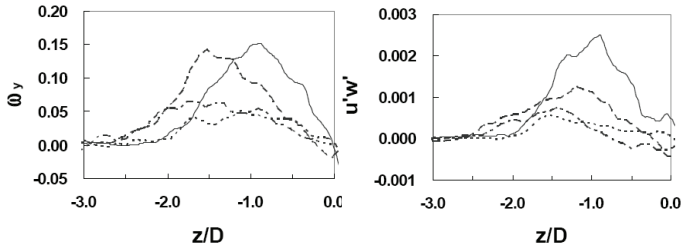

(a) (b)

Figure 10. The profiles of (a) mean y-vorticity (ω_y), at x/D=11 and y/D=2 (—), x/D=19 and y/D=2 (– – –), x/D=28 and y/D=3 (……) and x/D=36 and y/D=3 (-.-.-.-); (b) mean shear stress (u´w´), at x/D)=11 and y/D=2 (—), x/D=19 and y/D=2 (– – –), x/D=28 and y/D=3 (……), and x/D=36 and y/D=3 (-.-.-.-)

Double rollers are responsible for maintaining the correlation between the streamwise and lateral velocity fluctuations, with correlation being largest at the center plane of the structure [33]. The profiles of normalized shear stress (u´v´) at several downstream locations on wake center line are shown in Fig. 11. The shear stress peaks close to the wake formation length at x/D=3, and then decreases as x/D increases. Again, the input of momentum by the high velocity flow in the gap seems evident.

The Fig. 12 shows that the wake thickness and growth rate in the current discontinuous cylinder case are both larger than for the continuous cylinder wake. The Dumax and Ducl are the maximum velocity deficit and the wake centerline velocity deficit respectively, at that downstream station.

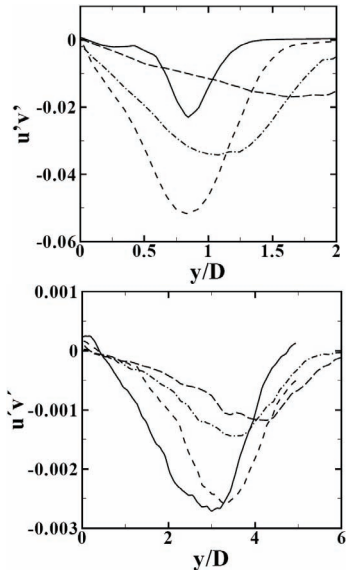

(a) (b)

Figure 11. The profiles of mean shear stress (u´v´) at (a) x/D=1.5 (—), x/D=3 (----), x/D=5 (-.-.-.-) and x/D=8 (– – –); (b) x/D)=26 (—), x/D=32 (----), x/D=44 (-.-.-.-),x/D=56 (– – –)

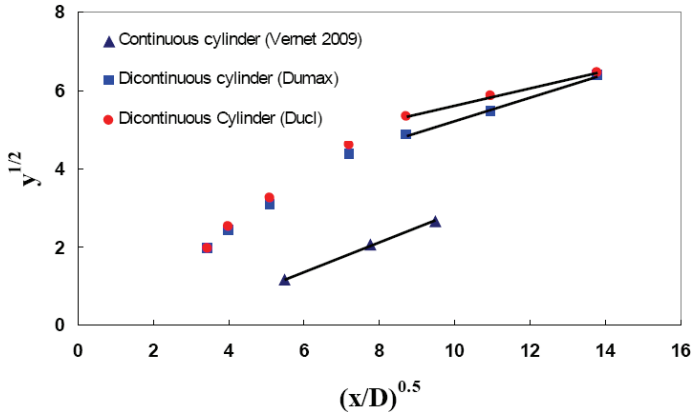

Figure 12. Variation of the wake half-width with streamwise location for both the discontinuous and continuous cylinder

Spanwise variation of the wake

The comparison of the wake behind a cylinder piece and in the gap region is shown below with the profiles of streamwise rms velocity fluctuations (Fig. 13) and spectra (Fig. 14). Close to the cylinder the mean flow is far from uniform in the span-wise direction but at x/D=190 the flow is uniform on spanwise direction, probably this is because of the 3D structures formed in the near wake are diffused to span-wise direction as they advect to downstream.

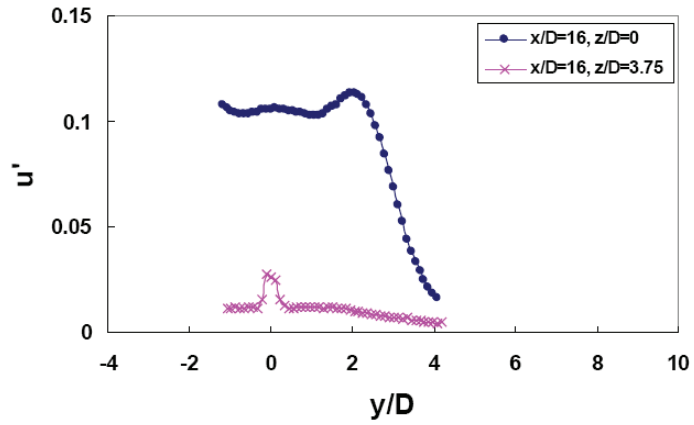

(a)

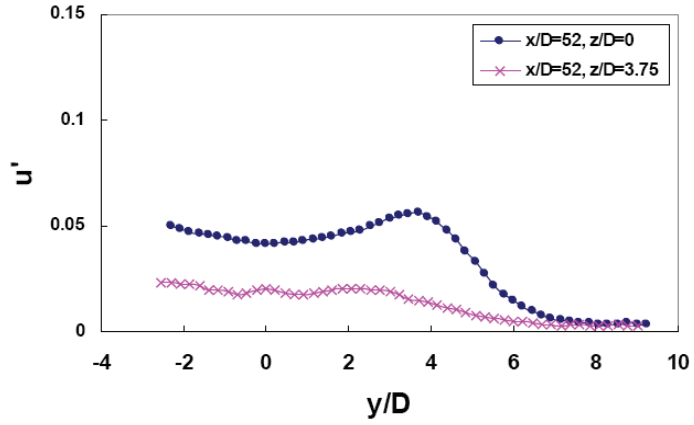

(b)

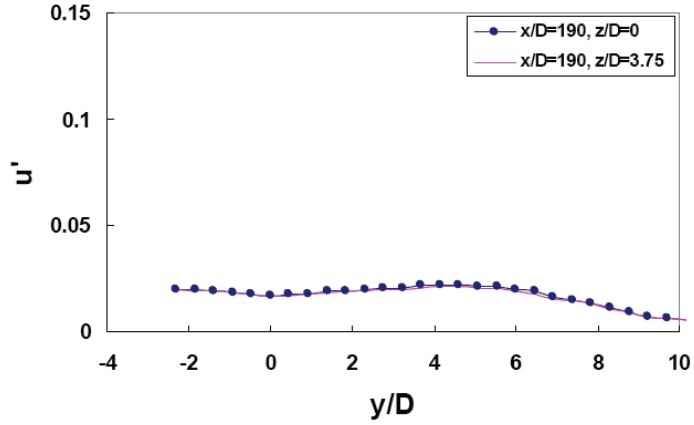

(c)

Figure 13. Comparison of the profiles of streamwise rms velocity fluctuations in the planes z/D=0 and z/D=3.75, at (a) x/D=16 (b) x/D=52, (c) x/D=190

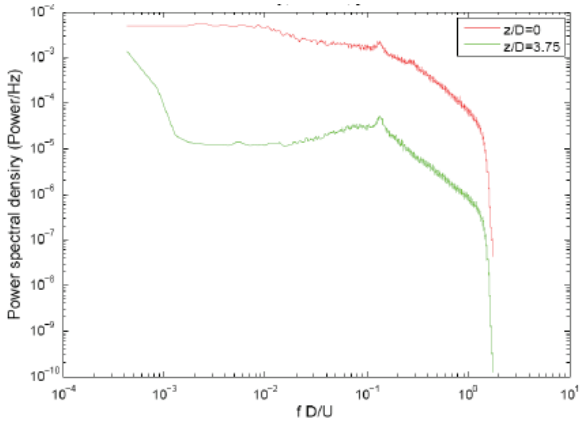

(a)

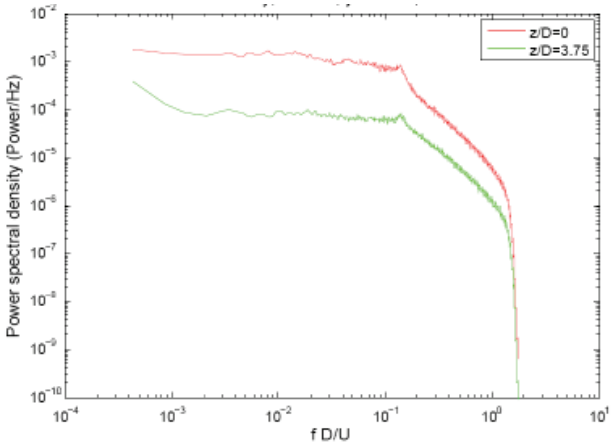

(b)

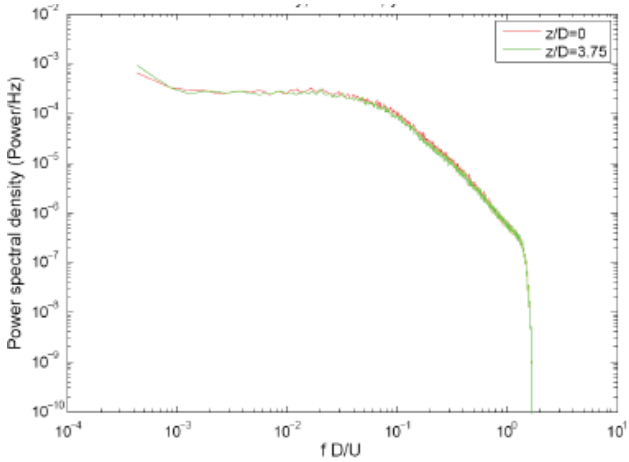

(c)

Figure 14. Comparison of the spectra in the planes z/D=0 and z/D=3.75, at (a) x/D=16 (b) x/D=52 (c) x/D=190

CONCLUSIONS

The effect of inflow conditions on the near wake and far wake structures behind a discontinuous cylinder, at Reynolds numbers Re=10000 and 4000 was investigated experimentally. The flow statistics such as mean velocities, rms velocity fluctuations, mean Reynolds shear stress and mean z-vorticity of the discontinuous cylinder have been compared with the corresponding data for an infinite cylinder wake. The wake bubble behind the segments of the discontinuous cylinder is significantly longer than that for the infinite cylinder, i.e., the formation length is longer. This delay shedding may be related to the converging streamlines in the wake from ends of the cylinder due to the inflow of high momentum fluid through the gaps. The wake width of the discontinuous cylinder is much wider and grows faster than that for the infinite cylinder. The velocity deficit is larger in the near wake region, but as the wake grows downstream it recovers quickly. Footprints of double-roller vortices have been unambiguously identified on the horizontal planes in the wake of the discontinuous cylinder. The non-dimensional shedding frequency (Strouhal number) of the double rollers in the wake is 0.14. The wake is far from uniform on spanwise axis at close to the cylinder, but at downstream station x/D=190 it is uniform on spanwise direction. The spread rate for the discontinuous cylinder is substantially larger than the continuous cylinder.

ACKNOWLEDGMENTS

The current study was supported by the grants FIS2005-07194 and CTQ2008-04857/PPQ (MEC & MICINN, Spain), and 2005SGR-00735 and 2009SGR-01529 (DURSI, Generalitat de Catalunya). Francesc Giralt acknowledges the Distinguished Researcher Award, Generalitat de Catalunya. G.A. Kopp gratefully acknowledges the support of the Canada Research Chairs Program.

REFERENCES

[1] Townsend, A. A., 1976, "The structure of turbulence shear flow," 2nd edn. Cambridge University Press.

[2] Bevilaqua, P. M., and Lykoudis, P. S., 1977, "Some observation on the mechanisms of entrainment," AIAA Journal, 15, pp. 1194-1196.

[3] Prandtl, L., and Tietjens, O. G., 1934, "Fundamentals of hydro- and aeromechanics," United engineers Trustees.

[4] Sreenivasan, K. R., Ramshankar, R., and Meneveau C., 1989, "Mixing, entrainment and fractal dimensions of surfaces in turbulent flows," Proc. R. Soc. Lond. A, 421, pp. 79-108.

[5] Caulfield, C. P., and Peltier, W. R., 2000, "The anatomy of mixing transition in homogeneous and stratified free shear layers," Journal of Fluid Mechanics, 413, pp. 1-47.

[6] Townsend, A. A., 1966, "The mechanism of entrainment in free turbulent flows, Journal of Fluid Mechanics," 26, pp. 689-715.

[7] Mathew, J., and Basu, A. J., 2002, "Some characteristics of entrainment at a cylindrical turbulence boundary," Physics of Fluids, 14, pp. 2065-2072.

[8] Westerweel, J., Fukushima, C., Pedersen, J. M., and Hunt, J. C. R., 2005, "Mechanics of the turbulent and non-turbulent interface of a jet," Physical Review Letters, 17, pp. 174501.

[9] Gerrard, J. H., 1967, "Experimental investigation of separated boundary layer undergoing transition to turbulence," Physics of Fluids, 10, pp. S98-100.

[10] Roshko, A., and Fiszdon, W., 1969, "On the persistence of transition in the near wake," Problems of Hydrodynamics and Continuum Mechanics," pp. 606-616. SIAM

[11] McCroskey, W. J., 1977, "Some current research in unsteady fluid dynamics – the 1976 freeman scholar lecture," Journal of Fluids Engineering, 99, pp. 8-39.

[12] Zdravkovich, M. M., 1990, "Conceptual over view of laminar and turbulent flows past smooth and rough cylinders," Journal of Wind Engineering and Industrial Aerodynamics, 33, pp. 53-62.

[13] Williamson, C. H. K., 1996, "Vortex dynamics in a cylinder wake," Annual Review of Fluid Mechanics, 28, pp. 477-539.

[14] Norberg, C., 2003, "Fluctuating lift on a circular cylinder: review and new measurements," Journal of Fluids and Structures, 17, pp. 57-96.

[15] Dong, S., Karniadakis, G. E., Ekmekci, A., and Rockwell, D., 2006, "A combined direct numerical simulation – particle image velocimetry study of the turbulent near wake," Journal of Fluid Mechanics, 569, pp. 185-207.

[16] Bearman, P. W., and Tombazis, N., 1993, "The effects of 3-dimensional imposed disturbances on bluff-body near wake flows," Jounal Wind Engineering and Industrial Aerodynamics, 49(1-3), pp. 339-349.

[17] Bearman, P. W., and Owen, J. C., 1998, "Reduction of bluff-body drag abd suppression of vortex shedding by the introduction of wavy separation lines," Jounal of Fluids and Structures, 12, pp. 123-130.

[18] Darekar, R. M., and Sherwin, S. J., 2001, "Flow past a bluff body with a wavy stagnation face," Journal of Fluids and Structures, 15(3-4), pp. 587-596.

[19] Lam, K., Wang, F. H., Li, J.Y., and So, R. M. C., 2004, "Experimental investigation of the mean and fluctuating forces of wavy (varicose) cylinders in a cross-flow," Journal of Fluid and Structures, 19(3), pp. 321-334.

[20] Wu, S. J., Miau, J. J., Hu, C. C., and Chou, J. H, 2005, "On low-frequency modulations and three-dimensionality in vortex shedding behind a normal plate," Journal of Fluid Mechanics, 526, pp. 117-146.

[21] Lee, S. J., and Nguyen, A. T., 2007, "Experimental investigation on wake behind a wavy cylinder having sinusoidal cross-sectional area variation," Fuid Dynamics Research, 39(4), pp. 292-304.

[22] Ling, G.. C., and Lin, L. M., 2008, "A note on the numerical simulations of flow past a wavy square-section cylinder," Acta Mechanica Sinica, 24(1), pp. 101-105.

[23] Ferré, J. A., and Giralt, F., 1988, “Pattern recognition analysis of the velocity field in plane turbulent wakes,” Journal of Fluid Mechanics, 198, pp. 27-64.
[24] Giralt, F., and Ferré, J. A., 1993, “Structure and flow pattern in turbulent flow,” Physics of Fluids, A5, pp. 1783-1789.
[25] Vernet, A., Kopp, G.. A., Ferré, J. A., and Giralt, F., 1999, “Three-dimensional structure and momentum transfer in a turbulent cylinder wake,” Journal of Fluid Mechanics, 394, pp. 303-337.
[26] Kopp, G.. A., Giralt, F., and Keffer, J. F, 2002, “Entrainment vortices and interfacial intermittent turbulent bulges in a plane turbulent wake,” Journal of Fluid Mechanics, 469, pp. 49-70.
[27] Dimotakis, P. E., 2000, “The mixing transition in turbulent flows,” Journal of Fluid Mechanics, 409, pp. 69-98.
[28] Norberb, C., 1998, “LDV-measurements in the near wake of a circular cylinder, Advances in understanding of bluff body wakes and vortex induced vibrations,” Washington DC, June 1998.
[29] Bloor, S., 1966, “The transition to turbulence in the wake of a circular cylinder, Journal of Fluid Mechanics,” 19, pp. 290-304.
[30] Woo, H. G., Cermak, J. E., and Peterka, J. A., 1983, “On vortex locking-on phenomenon for a cable in linear shear flow,” Journal of Wind Engineering and Industrial Aerodynamics, 14, pp. 289-300.
[31] Norberg, C., 1986, “Interaction between freestream turbulence and vortex shedding for a single tube in cross flow,” Journal of Wind engineering And Industrial Aerodynamics, 23, pp. 501-514.
[32] Govardhan, R., and Williamson, C. H. K., 2001, “Mean and fluctuating velocity fields in the wake of a freely vibrating cylinder,” Journal of Fluids and Structures, 15, pp. 489-501.
[33] Vernet, A., Kopp, G. A., Ferré, J. A., and Giralt F., 1997, “Simultaneous velocity and temperature patterns in the far region of a turbulent cylinder wake,” Journal of fluids Engineering, 119, pp. 463-466.
[34] Vernet, A., 2009, Private communication